A Fast Algorithm for the Calculation of Transonic Flow over Wing/Body Combinations

T. J. Baker* and C. R. Forsey*
Aircraft Research Association Limited, Bedford, England

A method to calculate transonic flows over wing/body combinations using the full potential equation is described. A sequence of transformations is used to transform the flowfield to the inside of a circular cylinder and the flow equation is solved in this space by a finite difference technique. A new approximate factorization algorithm has been developed to obtain rapid convergence several times faster than a conventional relaxation method used previously. Results are presented for a realistic configuration, showing the relative convergence rates of the two methods and comparing computed with experimental results.

Introduction

APPROXIMATE factorization has proved to be a reliable and effective technique for improving the convergence of transonic flow methods. The development of the AF2 algorithm[1] for solving the transonic small perturbation (TSP) equation was soon followed by implicit schemes for the full potential equation. Holst's version of the AF2 algorithm,[2,3] which was developed for the potential equation in conservative form, achieves rapid convergence over a wide range of difficult flow conditions. He has successfully extended this scheme to a three-dimensional algorithm[3] which has been used to compute transonic flow over a wing in a channel. Work aimed at solving the full potential equation in its nonconservative or quasilinear form has led to an alternative approximate factorization scheme.[4,5] This algorithm known as AF3 is also an extension of the AF2 factorization presented in Ref. 1. Although the AF3 method was developed independently of Holst's work, it is essentially the same as his scheme when applied to incompressible flow. For compressible flow and particularly in their treatment of supersonic regions, these two schemes differ. The AF3 algorithm has achieved rapid and reliable convergence over a wide range of flow conditions and for various types of coordinate mesh.

In this paper we describe an extension of the AF3 method to calculate flows over wings and wing/body combinations. A relaxation code[6] for this geometric configuration has been available for several years and has been used extensively for the calculation of transonic flow over a variety of wings and wing/body combinations. However, the convergence of a relaxation method is slow and there is often some uncertainty as to whether a converged result really has been reached. Indeed, for some difficult cases, one can easily be misled into believing that convergence has been achieved, only to find several hundred iterations later that the predicted pressure distribution has changed by a significant amount. In our experience, the convergence of approximate factorization methods is not only faster than relaxation but more reliable. The coordinate mesh that is employed and the finite difference approximations to the potential equation are the same in both the relaxation and approximate factorization codes. However, the replacement of a relaxation algorithm by our approximate factorization technique has led to a four- or fivefold improvement in convergence rate.

Presented as Paper 81-1015 at the AIAA 5th Computational Fluid Dynamics Conference, Palo Alto, Calif., June 22-23, 1981; submitted June 29, 1981; revision received May 11, 1982.

*Senior Project Supervisor.

Grid Generation

The choice of a suitable computing grid is an important factor in the development of a three-dimensional transonic code. Such grids are usually generated by mapping the flowfield into some computational space where a uniformly spaced grid can be taken. The best known approach for wing/body combinations is that of Jameson[7] who uses a conformal transformation to remove the body, followed by a square root transformation with shearing to unwrap the wing sections into the upper half-plane. Recently, numerically generated grids capable of dealing with general noncircular bodies and other complex configurations have become available.[8,9]

The approach adopted here is somewhat different and utilizes the excellent two-dimensional grid produced by conformally mapping an airfoil section into a circle.[10] In essence the flowfield surrounding the wing/body configuration is mapped onto the interior of a circular cylinder (see Fig. 1) in such a way that part of the cylinder corresponds to the wing surface and part of one end of the cylinder corresponds to the body surface. The remainder of the cylinder's surface corresponds to branch cuts, plane of symmetry, and outboard infinity. The coordinate transformations are performed using a separate mapping program and the transformation derivatives and metric coefficients are written onto a disk file for later access by the flow program. This added flexibility has proved quite advantageous in modifying the method to use an AF flow algorithm as the mapping program remains essentially unchanged.

The grid generation can be broken down into a series of steps. Initially, each body cross section in physical space (x,y,z) is mapped to part of the plane of symmetry in intermediate space (X,Y,Z) by the conformal transformation

$$\omega = \zeta + (R^2/\zeta)$$

where $\zeta = z + iy$ and $\omega = Z + iY$. This mapping takes the circle

$$y^2 + z^2 = R^2$$

into the slit $Y=0$, $|Z| \leq 2R$. It follows that only circular bodies can be modeled, although the radius R may vary with x and the wing may be mounted at any height on the body. As Caughey and Jameson[11] point out, this procedure for treating the body leads to a grid which is not everywhere aligned with the body surface. In practice, however, this has not had any noticeable effect on the predicted pressures for the wide range of cases we have considered.

The resulting, slightly distorted wing in intermediate space is mapped to a cylinder in computational (r,η,θ) space by first

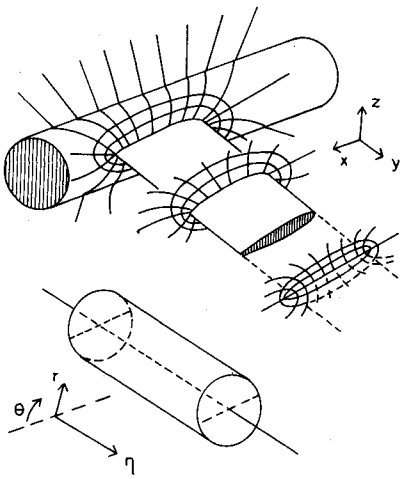

Fig. 1 Computing grid.

smoothly extending the planform from wing tip to infinity as a branch cut. A spanwise transformation $\eta = \eta(Y)$ is used to map outboard infinity to $\eta = 1$ and to define a series of sections through the wing and branch cut with packing toward root, tip, and any cranks (i.e., slope discontinuities in the leading and trailing edges of the wing planform).

Each section is mapped conformally to the inside of a circle. Sections through the branch cut outboard of the tip are slits that are mapped analytically using the inverse of the body transformation, viz.,

$$\tau = \sigma + (1/\sigma)$$

where

$$\tau = X + iZ \text{ and } \sigma = re^{i\theta}$$

Sections through the wing are mapped numerically using an iterative technique in which the mapping derivative $d\tau/d\sigma$ is expressed as a Fourier series

$$\frac{d\tau}{d\sigma} = (1-\sigma)^{1-\epsilon/\pi} \exp\left[\sum_{k=0}^{N} C_k \sigma^k\right]$$

The coefficients C_k are evaluated by a fast Fourier transform algorithm. The extra term $(1-\sigma)^{1-\epsilon/\pi}$, where ϵ is the trailing-edge angle, has the effect of removing the mapping singularity at the trailing edge.

As an extra refinement, an auxiliary transformation is applied to the r coordinate to compensate for the effects of wing sweep and taper on the outermost spanwise grid lines near the wing tip.

Difference Formulas

The flowfield around the wing/body combination is calculated by solving a finite difference approximation to the quasilinear form of the compressible potential equation. In transform coordinates (r, η, θ) the equation may be written

$$L\phi = C_{11}\phi_{rr} + C_{22}\phi_{\eta\eta} + C_{33}\phi_{\theta\theta} + C_{12}\phi_{r\eta} + C_{13}\phi_{r\theta} + C_{23}\phi_{\eta\theta} + D = 0 \tag{1}$$

where

$$C_{mn} = g^{mn} - v^m v^n / a^2 \tag{2}$$

and D contains all the lower-order terms. The contravariant components of the metric tensor g^{mn} and the contravariant velocity components v^m, v^n are standard tensor quantities, a the local speed of sound, and ϕ the perturbation potential.

We now introduce the discrete function $\phi_{i,j,k}$ corresponding to the continuous potential ϕ at the point $(i\Delta r, j\Delta\eta, k\Delta\theta)$ in computational space. The variable i runs from 1 to L, j runs from 1 to M, and k from 2 to N. In order to express difference approximations in a concise form, it is convenient to introduce the operators

$$\delta_r \phi_{i,j,k} = \phi_{i+\frac{1}{2},j,k} - \phi_{i-\frac{1}{2},j,k}$$

$$\overleftarrow{\delta}_r \phi_{i,j,k} = \phi_{i,j,k} - \phi_{i-1,j,k}$$

$$\overrightarrow{\delta}_r \phi_{i,j,k} = \phi_{i+1,j,k} - \phi_{i,j,k}$$

$$\delta_{rr}\phi_{i,j,k} \equiv \delta_r \delta_r \phi_{i,j,k} \equiv \overrightarrow{\delta}_r \overleftarrow{\delta}_r \phi_{i,j,k} = \phi_{i+1,j,k} - 2\phi_{i,j,k} + \phi_{i-1,j,k}$$

$$\mu_r \phi_{i,j,k} = \tfrac{1}{2}(\phi_{i+\frac{1}{2},j,k} + \phi_{i-\frac{1}{2},j,k})$$

with similar expressions for δ_η, δ_θ, etc.

In subsonic regions we can write the residual after n iteration cycles as

$$L\phi^n_{i,j,k} = \left(C_{11}\frac{\delta_{rr}}{\Delta r^2} + C_{22}\frac{\delta_{\eta\eta}}{\Delta\eta^2} + C_{33}\frac{\delta_{\theta\theta}}{\Delta\theta^2} + C_{12}\mu_r\mu_\eta\frac{\delta_r\delta_\eta}{\Delta r\Delta\eta} + C_{13}\mu_r\mu_\theta\frac{\delta_r\delta_\theta}{\Delta r\Delta\theta} + C_{23}\mu_\eta\mu_\theta\frac{\delta_\eta\delta_\theta}{\Delta\eta\Delta\theta}\right)\phi^n_{i,j,k} + D \tag{3}$$

In regions where the flow is supersonic a combination of centered and upwind differencing is employed in order to ensure computational stability. The coefficients in Eq. (1) can be written as

$$C_{mn} = C^c_{mn} + C^u_{mn}, \quad m = 1,2,3; \quad n = 1,2,3$$

where the superscript u refers to the contribution to the upwind differenced term and the superscript c denotes the centrally differenced contribution. Under a rotated difference scheme these two parts can be identified readily as

$$C^c_{mn} = g^{mn} - \frac{v^m v^n}{q^2}, \quad C^u_{mn} = \left(1 - \frac{q^2}{a^2}\right)\frac{v^m v^n}{q^2} \tag{4}$$

where q is the flow speed.

It follows that in supersonic regions, when all velocity components are positive, the residual can be written as

$$L\phi^n_{i,j,k} = \left(C^u_{11}\frac{\overleftarrow{\delta}_r\overleftarrow{\delta}_r}{\Delta r^2} + C^c_{11}\frac{\delta_{rr}}{\Delta r^2} + C^u_{22}\frac{\overleftarrow{\delta}_\eta\overleftarrow{\delta}_\eta}{\Delta\eta^2} + C^c_{22}\frac{\delta_{\eta\eta}}{\Delta\eta^2} + C^u_{33}\frac{\overleftarrow{\delta}_\theta\overleftarrow{\delta}_\theta}{\Delta\theta^2} + C^c_{33}\frac{\delta_{\theta\theta}}{\Delta\theta^2} + C^u_{12}\frac{\overleftarrow{\delta}_r\overleftarrow{\delta}_\eta}{\Delta r\Delta\eta} + C^c_{12}\mu_r\mu_\eta\frac{\delta_r\delta_\eta}{\Delta r\Delta\eta} + C^u_{13}\frac{\overleftarrow{\delta}_r\overleftarrow{\delta}_\theta}{\Delta r\Delta\theta} + C^c_{13}\mu_r\mu_\theta\frac{\delta_r\delta_\theta}{\Delta r\Delta\theta} + C^u_{23}\frac{\overleftarrow{\delta}_\eta\overleftarrow{\delta}_\theta}{\Delta\eta\Delta\theta} + C^c_{23}\mu_\eta\mu_\theta\frac{\delta_\eta\delta_\theta}{\Delta\eta\Delta\theta}\right)\phi^n_{i,j,k} + D \tag{5}$$

Following an idea of Krupp,[12] modifications are made to the central difference operators in supersonic regions to control the amount of artificial viscosity in the difference scheme. For example, the operator δ_{rr} is replaced by $\delta_{rr} - (1-\epsilon)\overleftarrow{\delta}_\theta\delta_{rr}$ with similar expressions for the other operators. Such control over the artificial viscosity improves the capture of weak, highly swept shocks. At trailing-edge points (and at leading-edge points outboard of the wing tip), the conformal mapping to a circle introduces mapping singularities. A special limiting form of the flow equation is then used in which C_{12}, C_{22}, and C_{23} are zero and the remaining coefficients assume a simplified form.

The difference scheme chosen is nonconservative which has been found to give consistently better agreement with experimental results. A partially conservative scheme based on the approach of Lock[13] is also available as a user option and may well be required when the viscous-inviscid interactive version becomes available.

In tensor form the appropriate contravariant velocity components are zero on all solid boundaries. The Kutta condition is applied as a jump in potential across the branch cut downstream of the trailing edge and continuity is applied across the branch cut outboard of the tip. Finally, since the Trefftz plane maps to a slit, the perturbation potential is set to zero everywhere at infinity.

Approximate Factorization Algorithm

Consider the general iterative scheme

$$N\Delta^n_{i,j,k} = \sigma L\phi^n_{i,j,k}$$

where $L\phi^n_{i,j,k}$ is the residual after n iteration cycles and $\Delta^n_{i,j,k}$ is the correction vector for cycle $n+1$ which is defined by

$$\Delta^n_{i,j,k} = \phi^{n+1}_{i,j,k} - \phi^n_{i,j,k}$$

The convergence rate of the iterative scheme depends on the choice of the iteration operator N. The requirement of fast stable convergence suggests the adoption of an implicit scheme that will ensure that all points in the flowfield are influenced by all other points in the course of each iteration. On the other hand, computational simplicity favors a scheme that involves only tridiagonal or bidiagonal matrix inversions. Approximate factorization methods satisfy these two aims by constructing N as a series of easily inverted factors. To illustrate this idea, we first consider Laplace's equation in two dimensions with respect to a Cartesian coordinate system,

$$\phi_{xx} + \phi_{yy} = 0$$

The residual corresponding to the usual centered difference approximation is

$$L\phi^n_{i,j} = \left(\frac{\delta_{xx}}{\Delta x^2} + \frac{\delta_{yy}}{\Delta y^2}\right)\phi^n_{i,j}$$

and the following AF2 factorization:

$$\left(-\alpha\frac{\vec{\delta_y}}{\Delta y} - \frac{\delta_{xx}}{\Delta x^2}\right)\left(\alpha + \frac{\overleftarrow{\delta_y}}{\Delta y}\right)\Delta^n_{i,j} = \sigma\alpha L\phi^n_{i,j} \tag{6}$$

will produce rapid convergence. This implicit factored scheme was first proposed by Ballhaus et al.[1] for solving the TSP equation and has been successfully extended to treat the full potential equation in both conservative[2,3] and nonconservative[4,5] forms.

This factorization is the basis of our extension to the three-dimensional AF3 scheme described subsequently. First, however, we shall present some results from two-dimensional approximate factorization theory. When an AF2 scheme is used on a stretched grid with varying aspect ratio, it can be shown that slow convergence can result unless the form of the factors is chosen correctly.[5,14,15] Consider, for example, a transformation to orthogonal curvilinear coordinates $X(x,y)$ and $Y(x,y)$ so that Laplace's equation becomes

$$g^{11}\phi_{XX} + g^{22}\phi_{YY} + D = 0 \tag{7}$$

The metric tensor components that appear in the preceding equation are defined as

$$g^{11} = X_x^2 + X_y^2, \qquad g^{22} = Y_x^2 + Y_y^2$$

and D contains the remaining first derivative terms that arise through the coordinate transformation. We introduce the generalized AF2 scheme

$$\left(-\alpha A_2\frac{\vec{\delta_Y}}{\Delta Y} - A_1\frac{\delta_{XX}}{\Delta X^2}\right)\left(B_1\alpha + B_2\frac{\overleftarrow{\delta_Y}}{\Delta Y}\right)\Delta^n_{i,j} = \sigma\alpha L\phi^n_{i,j} \tag{8}$$

where $L\phi^n_{i,j}$ is now the residual corresponding to Eq. (7) and the coefficients A_1, A_2, B_1, and B_2 are functions of X and Y which satisfy the conditions

$$A_1B_1 = g^{11}, \qquad A_2B_2 = g^{22} \tag{9}$$

but are otherwise arbitrary. A modal analysis[5,14] shows that optimum convergence is obtained when the coefficients are chosen to satisfy the following condition:

$$A_2/A_1 = B_2/B_1 = \sqrt{g^{22}/g^{11}} \tag{10}$$

If we take $B_1 = 1$ this leads to the following values for the remaining coefficients in Eq. (8):

$$A_1 = g^{11}, \quad A_2 = \sqrt{g^{11}g^{22}}, \quad B_2 = \sqrt{g^{22}/g^{11}} \tag{11}$$

Although condition Eq. (10) has been obtained for a simple model equation, it has been successfully exploited to generate optimum AF3 schemes for calculating transonic potential flow on highly stretched grids.[5,14]

To consider the implications in three dimensions, we return to Cartesian coordinates and write the residual corresponding to Laplace's equation as

$$L\phi^n_{i,j,k} = \left(\frac{\delta_{xx}}{\Delta x^2} + \frac{\delta_{yy}}{\Delta y^2} + \frac{\delta_{zz}}{\Delta z^2}\right)\phi^n_{i,j,k}$$

An appropriate extension of the two-dimensional AF2 scheme [Eq. (6)] is the following:

$$\left[\frac{1}{\alpha\Delta y}\left(\alpha - \Delta y\frac{\delta_{xx}}{\Delta x^2}\right)\left(\alpha - \Delta y\frac{\delta_{zz}}{\Delta z^2}\right) - \alpha\frac{E_y}{\Delta y}\right] \times \left(\alpha + \frac{\overleftarrow{\delta_y}}{\Delta y}\right)\Delta^n_{i,j,k} = \sigma\alpha L\phi^n_{i,j,k}$$

where E_y is the shift operator defined by

$$E_y\phi_{i,j,k} = \phi_{i,j+1,k}$$

This factorization is closely related to the approximate factorization algorithm proposed by Ballhaus and Steger[16] for the three-dimensional low-frequency TSP equation and is the basis of Holst's extension of the AF2 method to the three-dimensional conservative potential equation.[3] In this paper we seek a similar extension of the AF3 method[4,5] for solving the potential equation in nonconservative form. We now discuss the effect of varying grid aspect ratio and, following the ideas formulated in two dimensions, we look for a three-dimensional factorization that will work well on stretched grids. In place of Eq. (7) we consider

$$g^{11}\phi_{XX} + g^{22}\phi_{YY} + g^{33}\phi_{ZZ} + D = 0$$

and examine the following generalized factorization:

$$\left[\frac{A_2}{\alpha\Delta Y}\left(\alpha - \frac{A_1\Delta_Y}{A_2}\frac{\delta_{XX}}{\Delta X^2}\right)\left(\alpha - \frac{A_3\Delta_Y}{A_2}\frac{\delta_{ZZ}}{\Delta Z^2}\right) - \alpha\frac{A_2E_Y}{\Delta Y}\right] \times \left(\alpha B_1 + B_2\frac{\overleftarrow{\delta_Y}}{\Delta Y}\right)\Delta^n_{i,j,k} = \sigma\alpha L\phi^n_{i,j,k} \tag{12}$$

The coefficients should satisfy the conditions

$$A_1 B_1 = g^{11}, \quad A_3 B_1 = g^{33}$$

If we again choose $B_1 = 1$, it follows that

$$A_1 = g^{11}, \quad A_3 = g^{33}$$

The coefficients A_2 and B_2 should satisfy

$$A_2 B_2 = g^{22}$$

and like the earlier two-dimensional result, we look for a further condition that will determine the form of A_2 and B_2 leading to optimum convergence. Unfortunately, a modal analysis in three dimensions is extremely complicated and it is not clear whether one can obtain a fully satisfactory generalization of the two-dimensional theory. The argument that follows is by no means rigorous but does at least offer a guideline to the best coefficient choice. We first expand the two factors inside the main bracket on the left-hand side of Eq. (12) to give

$$\left[-\alpha\frac{A_2\vec{\delta}_Y}{\Delta Y} - g^{11}\frac{\delta_{XX}}{\Delta X^2} - g^{33}\frac{\delta_{ZZ}}{\Delta Z^2} + \frac{g^{11}\Delta Y}{\alpha}\frac{\delta_{XX}}{\Delta X^2}\frac{g^{33}}{A_2}\frac{\delta_{ZZ}}{\Delta Z^2}\right]$$

$$\times\left(\alpha + B_2\frac{\overleftarrow{\delta}_Y}{\Delta Y}\right)\Delta^n_{i,j,k} = \sigma\alpha L\phi^n_{i,j,k} \tag{13}$$

If we set the Z difference operator to zero, then the preceding expression reduces to the two-dimensional factorization, Eq. (8). Similarly, setting the X difference operator to zero leads to the equivalent two-dimensional form in terms of the independent variables Y and Z. It, therefore, seems reasonable to expect that a necessary condition for fast convergence is that the two-dimensional relation Eq. (10) should be satisfied both by the coefficients of X and Y and also by the coefficients of Z and Y. In other words, we require

$$A_2 \simeq \sqrt{g^{11}g^{22}}, \quad A_2 \simeq \sqrt{g^{33}g^{22}}$$

This will only be possible if

$$g^{11} \simeq g^{33} \tag{14}$$

Under an arbitrary three-dimensional coordinate transformation it is unlikely that this condition can be satisfied generally. It would, therefore, appear that the given condition amounts to a fairly severe restriction on the type of grid for which three-dimensional factorization schemes of the AF2 or AF3 type can achieve convergence rates comparable to those shown in two dimensions.

The computing grid that we have adopted for our calculation falls within the set of grids for which condition Eq. (14) can be satisfied. For the transformation in each $\eta = \text{const}$ plane is achieved by a conformal mapping to the computational variables r and θ. We can then identify dr with dX, $rd\theta$ with dZ, and $d\eta$ with dY. If the Y coordinate lines are orthogonal to the (X,Z) planes, then it follows that

$$g^{11} = g^{33} = r^4/H^2$$

where H is the mapping modulus for the transformation from the exterior of each wing section to the outside of a circle. In general, only the X and Z coordinates, which correspond to the conformally mapped variables, will be orthogonal and the Y coordinate line will be inclined to the (X,Z) planes. In this case g^{11} and g^{33} will not be equal but we can expect that both these metric components will be $0(r^4/H^2)$. The value of the metric component g^{22} will depend strongly on the stretching applied in the spanwise direction and its variation will be essentially independent of the behavior of g^{11} and g^{33}. If we, therefore, select

$$A_2 = (r^2\sqrt{g^{22}}/H)$$

and, hence,

$$B_2 = (H\sqrt{g^{22}}/r^2)$$

we can construct a factorization that, at first sight, would appear well suited to our coordinate system. This particular scheme has been tested but produced only very slow convergence. The reason for this disappointing result can probably be blamed on the presence of the term

$$\frac{g^{11}\Delta Y}{\alpha}\frac{\delta_{XX}}{\Delta X^2}\frac{g^{33}}{A_2}\frac{\delta_{ZZ}}{\Delta Z^2}$$

which appears in the first factor of Eq. (13) but whose influence was neglected in our discussion of optimum coefficient choice. The spanwise stretching that brings infinity outboard of the wing tip to a finite position in computational space produces a sparse distribution of points at large distances outboard of the tip. This leads to small values of g^{22} and, hence, small values of A_2 in this region. It follows that the term just noted becomes large and it is perhaps to be expected that this will lead to a slow convergence rate.

We, therefore, try an alternative arrangement in which an r difference operator appears in the last factor. In subcritical regions of flow, the residual for the equation we wish to solve is given by Eq. (3) with the coefficients C_{mn} defined by the expression Eq. (2). This expression involves centered difference approximations for the second derivatives of ϕ and we therefore construct the following three-dimensional factorization:

$$\left[\frac{\mu}{\alpha}\left(\alpha - \frac{C_{22}\delta_{\eta\eta}}{\mu\Delta\eta^2}\right)\left(\alpha - \frac{C_{33}\delta_{\theta\theta}}{\mu\Delta\theta^2}\right) - \alpha\mu E_r\right]$$

$$\times\left(\alpha + \frac{g^{11}\overleftarrow{\delta}_r}{\mu\Delta r^2}\right)\Delta^n_{i,j,k} = \sigma\alpha L\phi^n_{i,j,k} \tag{15}$$

The term μ is defined by

$$\mu = \frac{g^{11}}{r(g^{22})^{\nu}\Delta r}$$

and the expression $r(g^{22})^{\nu}$ in the denominator of μ is an allowance for grid stretching effects. The exponent ν is a user defined constant that usually takes the value $\nu = 0.1$. The results shown later have all been computed using the factored difference scheme Eqs. (15) and (16) with the preceding form for μ. It is, however, quite possible that a more careful choice of μ would lead to better convergence rates than those presented in the next section.

In regions where the flow is locally supersonic, the factorization must be modified to incorporate an upwind differenced contribution. This modification is a straightforward extension of the approach used in the two-dimensional AF3 scheme.[4,5] When the velocity components v^2 and v^3 are both positive, the factorization is written as

$$\left[\frac{\mu}{\alpha}\left(\alpha - \frac{C^c_{22}}{\mu}\frac{\delta_{\eta\eta}}{\Delta\eta^2} - \frac{C^u_{22}}{\mu}\frac{\overleftarrow{\delta}_\eta}{\Delta\eta^2}\right)\left(\alpha - \frac{C^c_{33}}{\mu}\frac{\delta_{\theta\theta}}{\Delta\theta^2}\right.\right.$$

$$\left.\left. - \frac{C^u_{33}}{\mu}\frac{\overleftarrow{\delta}_\theta}{\Delta\theta^2}\right) - \alpha\mu E_r\right]\left(\alpha + \frac{g^{11}\overleftarrow{\delta}_r}{\mu\Delta r^2}\right)\Delta^n_{i,j,k} = \sigma\alpha L\phi^n_{i,j,k} \tag{16}$$

When v^2 is negative, the term $-(C^u_{22}\overleftarrow{\delta}_\eta/\mu\Delta\eta^2)$, is replaced by $+(C^u_{22}\overrightarrow{\delta}_\eta/\mu\Delta\eta^2)$ with a similar change in the second factor

when $v^3 < 0$. The application of this algorithm proceeds in three steps and follows a very similar sequence to that described by Holst[3] for his fully-conservative code. Thus, Eq. (15) is solved as follows:

Step 1

$$\left(\mu - \frac{C_{22}}{\alpha}\frac{\delta_{\eta\eta}}{\Delta\eta^2}\right)G^n_{j,k} = \sigma\alpha L\phi^n_{i,j,k} + \alpha\mu F^n_{i+1,j,k}$$

Step 2

$$\left(\alpha - \frac{C_{33}}{\mu}\frac{\delta_{\theta\theta}}{\Delta\theta^2}\right)F^n_{i,j,k} = G^n_{j,k}$$

Step 3

$$\left(\alpha + \frac{g^{11}}{\mu}\frac{\overleftarrow{\delta_r}}{\Delta r^2}\right)\Delta^n_{i,j,k} = F^n_{i,j,k}$$

$G^n_{j,k}$ is an intermediate two-dimensional array of values stored on a given $r=$const surface. $F^n_{i,j,k}$ is a further intermediate result that is required at each grid point. Steps 1 and 2 are carried out on successive $i=$const planes, starting with the maximum i value at the wing surface and proceeding in the direction of decreasing r toward infinity in the radial or r direction.

For the initial set of inversions at the wing surface or $i=L$ plane, we require the values of $F^n_{L+1,j,k}$. These are taken to be zero, which is a boundary condition consistent with the final steady-state solution. The boundary conditions

$$G^n_{M,k} = 0 \text{ and } \left(\frac{\partial G}{\partial \eta}\right)_{1,k} = 0$$

are used in the tridiagonal inversion for step 1. The first of these is consistent with the assumption of zero perturbation potential at outboard infinity; the second corresponds to the Neumann boundary condition arising from the flow tangency requirement on the plane of symmetry at the wing root.

In solving the tridiagonal system for step 2 we need to take account of the periodicity in the θ direction as well as the jump in circulation on crossing the $\theta=0$ line. We solve for $F_{i,j,k}$ with k running from 2 to N. The line $k=2$ is the $\theta=0$ line and $k=N$ is the line $\theta=2\pi-\Delta\theta$. If we write the tridiagonal system for step 2 as

$$a_k F^n_{i,j,k+1} + b_k F^n_{i,j,k} + c_k F^n_{i,j,k-1} = d_k, \quad k=2\ldots N$$

we find, from step 3 of the algorithm that

$$F^n_{i,j,1} = \left(\alpha + \frac{g^{11}}{\mu}\frac{\overleftarrow{\delta_r}}{\Delta r^2}\right)\Delta^n_{i,j,1} = \left(\alpha + \frac{g^{11}}{\mu}\frac{\overleftarrow{\delta_r}}{\Delta r^2}\right)(\Delta^n_{i,j,N} - \Delta\Gamma^n_j)$$

where $\Delta\Gamma^n_j = \Gamma^{n+1}_j - \Gamma^n_j$. Thus,

$$F^n_{i,j,1} = F^n_{i,j,N} - \alpha\Delta\Gamma^n_j$$

It follows that for $k=2$ we obtain the difference equation

$$a_2 F^n_{i,j,3} + b_2 F^n_{i,j,2} + c_2 F^n_{i,j,N} = d_2 + c_2\alpha\Delta\Gamma^n_j$$

Similarly, for $k=N$ we get the following equation.

$$a_N F^n_{i,j,2} + b_N F^n_{i,j,N} + c_N F^n_{i,j,N-1} = d_N - a_N\alpha\Delta\Gamma^n_j$$

The new values of circulation Γ^{n+1}_j are not known at this stage and so we follow Holst[2] in extrapolating from previous iteration levels. Thus, we set

$$\Delta\Gamma^n_j \equiv \Gamma^{n+1}_j - \Gamma^n_j = 2\Gamma^n_j - 3\Gamma^{n-1}_j + \Gamma^{n-2}_j$$

Finally, step 3 is a straightforward series of bidiagonal inversions for which the boundary condition is

$$\Delta^n_{1,j,k} = 0$$

for $j=1$ to M and $k=2$ to N. This condition corresponds to the assumption of zero perturbation potential at infinity.

The acceleration parameters are varied between a maximum value $\alpha_h = 20$ and a minimum value $\alpha_l = 1$. Following Ballhaus et al.[1] we use a geometric sequence of parameters. The relaxation parameter is usually given the value $\sigma = 1$.

Results

The first example we consider is a panel wing, mounted on an infinitely long body of circular cross section. Each wing section has a NACA 0012 profile; the planform and cross section are shown in Fig. 2. Several computations have been carried out with this geometry for both wing alone and wing/body using a grid of $10\times20\times64$ points in the r, η, θ directions, respectively. The computed pressure distribution at six sections over the wing alone is presented in Fig. 3 for a supercritical case in which the freestream Mach number is 0.9 and the incidence 2 deg. It can be seen that there is a fairly extensive region of supersonic flow over the wing surface terminated by a strong shock.

In Fig. 4 we present convergence histories of the relaxation and approximate factorization computations. We have plotted $|R|$, the maximum absolute value of the residual normalized by its initial value, against equivalent relaxation iterations (ERI). For both wing alone and wing/body computations, relaxation shows a slow but steady reduction in residual. The convergence rate of the approximate factorization calculation for the wing alone is considerably faster, achieving a residual reduction of three orders of magnitude after the equivalent of 160 relaxation iterations.

The convergence history of the approximate factorization computation for the wing/body is much slower. After an initial rapid reduction, the curve flattens out and the residual decreases at an even slower rate than the corresponding result for relaxation. The residual, however, is heavily weighted toward the high-frequency end of the error spectrum. Since relaxation is very effective against high-frequency errors, comparisons based on the value of the residual tend to give a favorable but misleading impression of relaxation convergence. If we consider a more practical indicator of convergence such as the growth in the number of supersonic

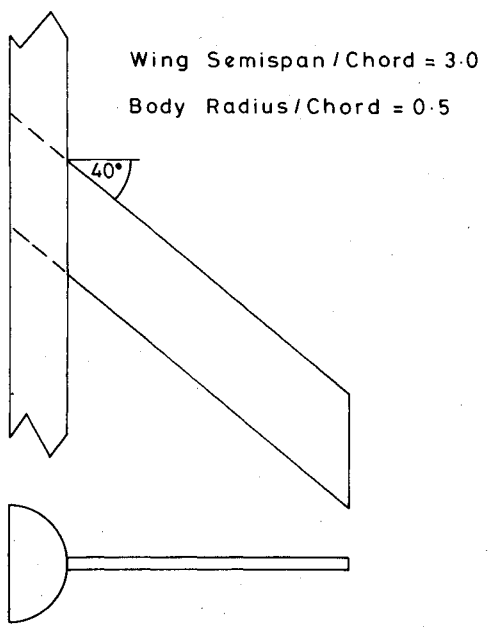

Fig. 2 Panel wing geometry.

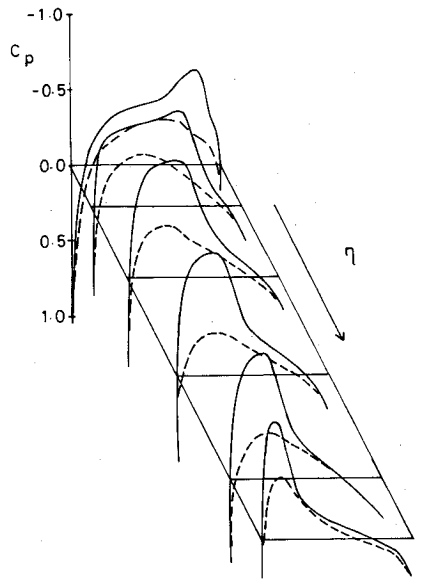

Fig. 3 Panel wing pressure distribution for wing alone.

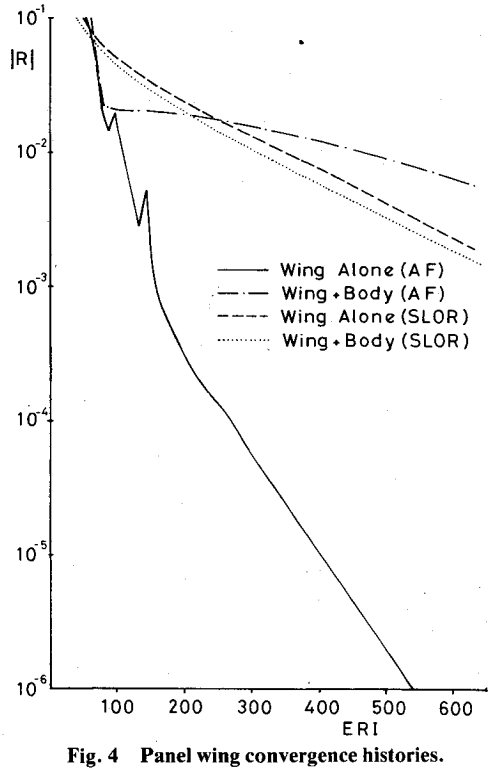

Fig. 4 Panel wing convergence histories.

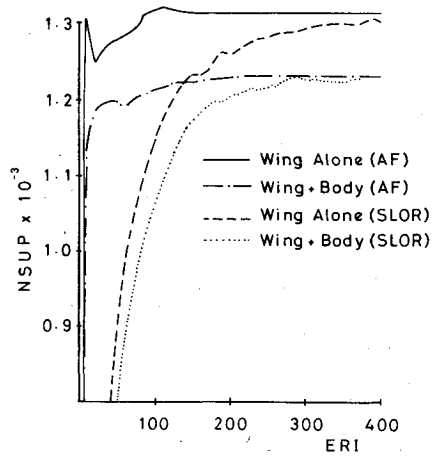

Fig. 5 Growth of supersonic region for panel wing, $M=0.9$, $\alpha=2$ deg.

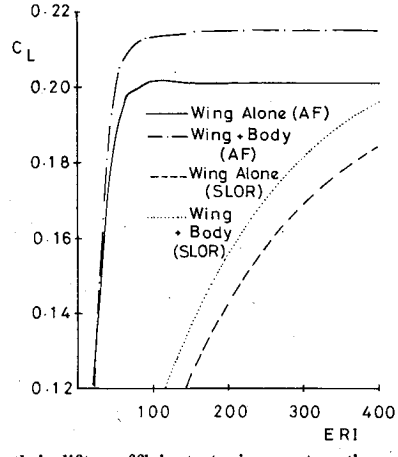

Fig. 6 Growth in lift coefficient at wing root section of panel wing, $M=0.9$, $\alpha=2$ deg.

points presented in Fig. 5, then it is clear that the approximate factorization scheme converges much more rapidly than relaxation for both the wing alone and the wing/body combination. A similar conclusion can be drawn by comparing the growth in lift coefficient at the wing root section. This information appears in Fig. 6 and it can again be seen that the convergence of the approximate factorization scheme is far superior to the corresponding relaxation result.

It should be noted that both the relaxation and approximate factorization codes have been run using the same grid and starting from the same initial conditions of zero perturbation potential everywhere. Both relaxation and approximate factorization converge to the same result, although it is clear from Fig. 6 that relaxation takes a very large number of iterations to reach the converged value of lift coefficient. In practice, one would normally use grid refinement to improve the convergence of a relaxation method and in the original relaxation code,[6] Forsey carries out computations on a sequence of three, increasingly fine grids. This usually ensures that the relaxation solution is close to the converged result after a relatively small number of iterations. Nevertheless, even with grid refinement, relaxation can still take a very large number of iterations to get within, say, 1% of the converged value of lift coefficient. This is in stark contrast to approximate factorization which quickly reaches the converged value.

Our second example is RAE wing A which has been proposed as an AGARD test case for comparison of three-dimensional theoretical methods.[17] The geometry of this wing/body combination is shown in Fig. 7. In Fig. 8 we compare theoretical and experimental pressure distributions at a freestream Mach number of 0.9 and an incidence of 1 deg. Note that in Fig. 8 the symbol η refers to physical distance along the wing measured from the wing root and does not refer, as previously used, to the spanwise position in computational space. Recently, Rizzi and Eriksson have developed a method to solve the Euler equations for wing/body combinations and, in Ref. 9, they present comparisons between their Euler solution and our potential solution for this case.

Figure 9 compares histories of relaxation and approximate factorization for a potential flow computation using a grid of $10\times24\times80$ points. The results are very similar to those presented in Fig. 4 with approximate factorization showing a considerable improvement over relaxation for the wing alone calculation. In this example we see that relaxation shows no

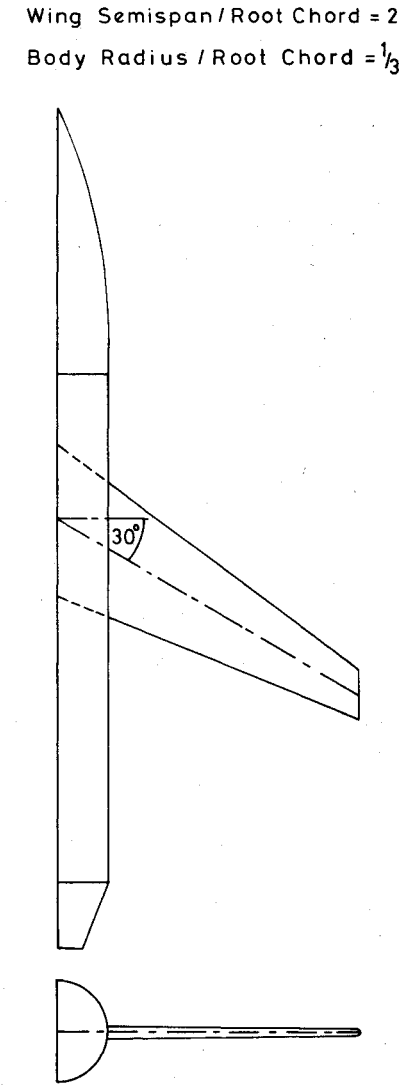

Fig. 7 RAE wing A plus body B2 geometry.

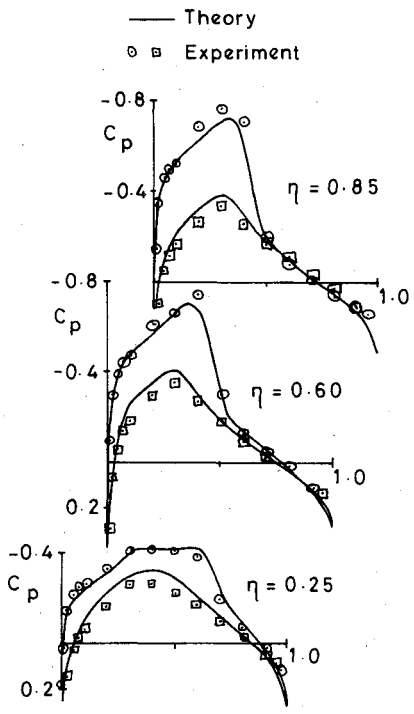

Fig. 8 RAE wing A plus body B2 wing pressures, $M = 0.9$, $\alpha = 1$ deg.

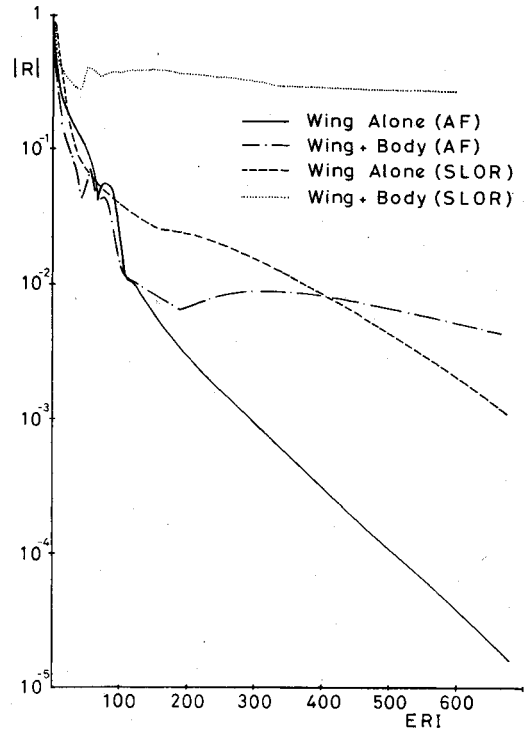

Fig. 9 RAE wing A plus body B2 convergence histories.

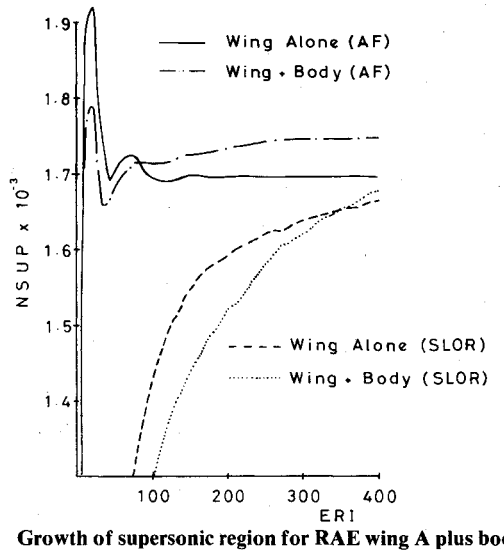

Fig. 10 Growth of supersonic region for RAE wing A plus body B2.

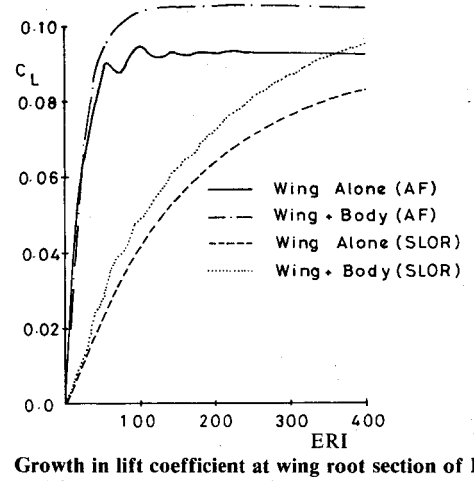

Fig. 11 Growth in lift coefficient at wing root section of RAE wing A plus body B2.

appreciable reduction in residual for the wing/body case. The difficulty lies at the trailing edge of the wing root section where the potential function alternates in value from one iteration to the next. The problem can be cured by applying under-relaxation in this region and the residual then decays at the same rate as it does for wing alone relaxation.

In the approximate factorization scheme no such treatment is applied at the trailing edge and does not appear to be necessary. On the other hand, the residual reduction for the approximate factorization computation on the wing/body soon levels out, as it did in the previous example. Here the difficulty appears to emanate from the far field region on the wake (i.e., $\theta = 0$ line) behind the wing root section.

A comparison of the growth of the supersonic region for both relaxation and approximate factorization for the wing/body case is presented in Fig. 10. Similarly, Fig. 11 compares the growth of lift coefficient at the wing root section which again gives a more realistic indication of the improvement that has been achieved by the introduction of our approximate factorization scheme.

Conclusions

The development of a three-dimensional approximate factorization scheme has led to useful improvements in the convergence rate of Forsey's[6] wing/body code and the results achieved so far are encouraging. Nevertheless, the convergence rates fall far short of the very rapid convergence demonstrated by two-dimensional approximate factorization routines.[3-5,14,15] This is probably caused to a large extent by the grid stretching that arises through mapping an infinite flowfield into a finite, computational space. For relaxation, which is an inherently slow iterative method, the convergence rate appears to be largely unaffected by grid stretching. However, it seems that the fast iterative techniques are much more sensitive. In two dimensions recent developments in both multigrid[18] and approximate factorization[5,14,15] have resolved this problem. It remains to be seen whether future developments can produce three-dimensional schemes that achieve comparable convergence rates for highly stretched grids such as the one considered in this paper.

Acknowledgment

This work has been carried out with the support of the Procurement Executive, Ministry of Defence.

References

[1] Ballhaus, W. F., Jameson, A., and Albert, J., "Implicit Approximate Factorization Schemes for the Efficient Solution of Steady Transonic Flow Problems," AIAA Paper 77-634, 1977.

[2] Holst, T. L., "An Implicit Algorithm for the Conservative, Transonic Full Potential Equation using an Arbitrary Mesh," AIAA Paper 78-1113, 1978.

[3] Holst, T. L., "A Fast, Conservative Algorithm for Solving the Transonic Full-Potential Equation," AIAA Paper 79-1456, 1979.

[4] Baker, T. J., "A Fast Implicit Algorithm for the Nonconservative Potential Equation," Open Forum Presentation at the AIAA 4th Computational Fluid Dynamics Conference, July 1979.

[5] Baker, T. J., "Potential Flow Calculation by the Approximate Factorization Method," *Journal of Computational Physics*, Vol. 42, July 1981, pp. 1-19.

[6] Forsey, C. R. and Carr, M. P., "The Calculation of Transonic Flow over Three-Dimensional Swept Wings using the Exact Potential Equation," *DGLR Symposium Transonic Configurations,* Bad Harzburg, DGLR Paper 78-064, June 1978.

[7] Jameson, A. and Caughey, D. A., "A Finite Volume Method for Transonic Potential Flow Calculations," AIAA Paper 77-635, 1977.

[8] Yu, N. J., "Grid Generation and Transonic Flow Calculations for Three-Dimensional Configurations," AIAA Paper 80-1391, July 1980.

[9] Rizzi, A. and Eriksson, L. E., "Transfinite Mesh Generation and Damped Euler Equation Algorithm for Transonic Flow around Wing-Body Configurations," AIAA Paper 81-999, June 1981.

[10] Bauer, F., Garabedian, P., Korn, D., and Jameson, A., *Supercritical Wing Sections II*, Lecture Notes in Economics and Mathematical Systems, Vol. 108, Springer-Verlag, Berlin, 1975.

[11] Caughey, D. A. and Jameson, A., "Progress in Finite-Volume Calculations for Wing-Fuselage Combinations," *AIAA Journal*, Vol. 18, Nov. 1980, pp. 1281-88; see also AIAA Paper 79-1513, July 1979.

[12] Krupp, J. A., "The Numerical Calculation of Plane Steady Transonic Flows past Thin Lifting Airfoils," Ph.D. Thesis, Dept. of Aeronautics and Astronautics, Univ. of Washington, 1971.

[13] Collyer, M. R., and Lock, R. C., "Prediction of Viscous Effects in Steady Transonic Flow past an Aerofoil," *Aeronautical Quarterly*, Vol. 30, Aug. 1979, pp. 485-505.

[14] Catherall, D., "Optimum Approximate Factorization Schemes for Two-Dimensional Steady Transonic Flows," AIAA Paper 81-1018, June 1981.

[15] Baker, T. J., "The Computation of Transonic Potential Flow," *VKI Lecture Series 1981-5 on Computational Fluid Dynamics*, von Karman Institute for Fluid Dynamics, Rhode-St-Genese, Belgium, March 1981.

[16] Ballhaus, W. F. and Steger, J. L., "Implicit Approximate Factorization Schemes for the Low Frequency Transonic Equation," NASA TM X-73082, 1975.

[17] *Experimental Data Base for Computer Program Assessment*, AGARD-AR-138, 1979.

[18] Jameson, A., "Acceleration of Transonic Potential Flow Calculations on Arbitrary Meshes by the Multiple Grid Method," AIAA Paper 79-1458, July 1979.